### Title

Electrical-biological hybrid system for carbon efficient isobutanol production




### Authors

Treece, Tanner R
Pattanayak, Santanu
Matson, Morgan M
et al.



### Publication Date

2023-09-01

### DOI

10.1016/j.ymben.2023.09.007

# Electrical-biological hybrid system for carbon efficient isobutanol production

Tanner R Treece[1ǂ], Santanu Pattanayak[1ǂ], Morgan M Matson[1], Mateo M Cepeda[1], Louise A Berben[1*], and Shota Atsumi[1*]

[1]Department of Chemistry, University of California, Davis, Davis, CA, 95616, USA

*To whom correspondence may be addressed: E-mail: satsumi@ucdavis.edu laberben@ucdavis.edu

ǂ These authors contributed equally

**Abstract**

We have developed an electrical-biological hybrid system wherein an engineered microorganism consumes electrocatalytically produced formate from $CO_2$ to supplement the bioproduction of isobutanol, a valuable fuel chemical. Biological $CO_2$ sequestration is notoriously slow compared to electrochemical $CO_2$ reduction, while electrochemical methods struggle to generate carbon-carbon bonds which readily form in biological systems. A hybrid system provides a promising method for combining the benefits of both biology and electrochemistry. Previously, *Escherichia coli* was engineered to assimilate formate and $CO_2$ in central metabolism using the reductive glycine pathway. In this work, we have shown that chemical production in *E. coli* can benefit from single carbon substrates when equipped with the RGP. By installing the RGP and the isobutanol biosynthetic pathway into *E. coli* and by further genetic modifications, we have generated a strain of *E. coli* that can consume formate and produce isobutanol at a yield of >100% of theoretical maximum from glucose. Our results demonstrate that carbon produced from electrocatalytically reduced $CO_2$ can bolster chemical production in *E. coli*. This study shows that *E. coli* can be engineered towards carbon efficient methods of chemical production.

**Keywords**: Electrical-biological hybrid system, metabolic engineering, electrocatalysis

Highlights

- Isobutanol yield is improved when reductive glycine pathway is installed.
- C1 substrates are incorporated into important intermediates.
- Electrocatalytically produced substrates without purification can be assimilated.

## Introduction

The current global climate crisis has been largely fueled by our reliance on fossil fuels, leading to unprecedented levels of greenhouse gases in the atmosphere (Chen et al., 2022). This ongoing crisis has driven an increased demand for sustainable chemical production from renewable sources. Developing methods to use atmospheric carbon dioxide for the production of chemical commodities has garnered particular attention in recent years as a solution that can both reduce current greenhouse gas levels and provide an alternative to petroleum-based chemistry (Barecka et al., 2021; Case and Atsumi, 2016). Biological systems of engineered microorganisms have been studied to either indirectly or directly use atmospheric $CO_2$ for the production of valuable chemical commodities (Case and Atsumi, 2016; Lynd et al., 1991). Traditional biological fermentation strategies perform indirect $CO_2$ sequestration by feeding sugar feedstocks sourced from various crops to heterotrophic microorganisms such as yeast or *Escherichia coli*. This methodology has the drawback of directly competing with the global food supply (Cheng et al., 2019). Using photosynthetic production systems for direct $CO_2$ reduction also has drawbacks such as slow growth and lower production rates compared to heterotrophic microbes (Case and Atsumi, 2016). Inorganic strategies for $CO_2$ sequestration have similarly been investigated and provide an efficient means to convert $CO_2$ into more useful single carbon molecules (Chen et al., 2020; Fernández-Caso et al., 2023; Goeppert et al., 2014; Loewen et al., 2017; Nitopi et al., 2019; Taheri et al., 2015). However, inorganic methods cannot efficiently create carbon-carbon bonds (Goeppert et al., 2014). These drawbacks to both biological production and inorganic $CO_2$ conversion have motivated research into various hybrid strategies where single carbon molecules produced from electrocatalytically reduced $CO_2$ are fed to biological hosts, providing a production platform that circumvents the aforementioned drawbacks (Tashiro et al., 2018; Bang et al., 2020; Döring et al., 2018; Lim et al., 2023). Here, in the model organism *E. coli* we built upon the reductive glycine pathway (RGP) and have shown that *E. coli* can efficiently convert the electrochemically relevant molecule, formate, into the value-added product, isobutanol, a gasoline substitute and a precursor for jet fuel and polymers when the *E. coli* strain is equipped with both the RGP and an isobutanol production pathway (Volanti et al., 2019; Wang and Tao, 2016).

In a previous study, the theorized RGP was shown to function effectively in *E. coli,* enabling growth in a serine auxotrophic strain (Tashiro et al., 2018). Other studies using a similar strategy to the RGP have shown that *E. coli* can be engineered to grow on formate and $CO_2$ alone, but the resultant chemoautotrophic *E. coli* suffers from slow growth and lower overall chemical production (Bang et al., 2020). One study hypothesized that intracellular NADH and NADPH levels contributed to the slower growth phenotype. Two genes encoding for variants of the enzyme formate dehydrogenase were installed to generate additional reducing equivalents, however, the engineered strain still lagged behind standard growth rates for *E. coli* (Bang et al., 2020).

The RGP requires two carbon inputs: formate and $CO_2$. In an electrocatalytic setting $CO_2$ can be reduced to formate, simplifying the carbon inputs for the RGP (Taheri et al., 2015; Tashiro et al., 2018). In a previous study, it was demonstrated that *E. coli* is capable of growing and assimilating $CO_2$ and formate in the cathode of an electrochemical bioreactor where $CO_2$ is readily converted to formate, reducing the carbon inputs down to $CO_2$ alone (Tashiro et al., 2018). The previous study required the use of the rare metal indium for the working electrode for the reduction of $CO_2$ to formate (Tashiro et al., 2018). In this study, we demonstrate that an iron carbonyl cluster can alternatively be used to reduce $CO_2$ to formate in the hybrid system. There are several benefits to using this iron-based catalysis compared to indium. Iron is Earth-abundant metal and the iron carbonyl cluster can perform catalysis for longer durations (Taheri et al., 2015). Additionally, this iron-based catalyst has the highest observed catalytic rates at neutral pH, making this catalyst ideal for a biological hybrid system (Taheri et al., 2015). Using a carbon electrode in the working compartment of the catalysis prevents the use an otherwise toxic metal electrode that impacts the overall health of the biocatalysis. The catalyst used in this study is highly stable and specific to formate production, as such it does not produce other side products such CO, $H_2$, oxalate, methanol, or formaldehyde making it superior to other catalysts in the context of electrical-biological systems (Taheri et al., 2015).

The downstream chemical of choice in this study, isobutanol, is a relevant polymer and jet fuel precursor (Atsumi et al., 2008b; Geleynse et al., 2018). Isobutanol production in *E. coli* is well established (Atsumi et al., 2008b). Connecting the RGP to isobutanol production provides an ideal signal for determining if the RGP is capable of incorporating formate and $CO_2$ into a biologically derived chemical product (Atsumi et al., 2008b). An important study for this field determined that the chemolithotrophic bacterium, *Ralstonia eutropha,* could produce isobutanol from electrochemically produced formate (Li et al., 2012). However, *R. eutropha* is an obligate aerobe and susceptible to damage from the reactive oxygen species that are generated in an electrocatalytic setting where oxygen is present. While isobutanol provides a robust indicator of *E. coli*'s ability to efficiently convert formate into a value-added chemical, many other chemical commodities can be generated using this system. Due to the ability of the RGP to incorporate formate and $CO_2$ into pyruvate, any downstream chemical production pathway that relies on intracellular pyruvate pools could potentially benefit from the RGP (Tashiro et al., 2018).

This study represents the ability of an electrical-biological hybrid system to provide a more renewable platform for chemical production in *E. coli* compared to traditional heterotrophic fermentations while also providing a more efficient method for $CO_2$ sequestration compared to Ribulose-1,5-bisphosphate carboxylase/oxygenase (RubisCO) based carbon capture.

## Methods

### Reagents

All enzymes involved in the molecular cloning experiments were purchased from New England Biolabs (NEB). All synthetic oligonucleotides were synthesized by Integrated DNA Technologies. Sanger Sequencing was provided by Genewiz from Azenta Life Sciences.

**Strains and Plasmids**

All strains and plasmids used in this study are listed in **Table 1** and **Table S1**, respectively. All oligonucleotides are listed in **Table S2**. Plasmids were constructed using sequence and ligation independent cloning (SLIC) (Jeong et al., 2012). The constructed plasmids were verified via Sanger Sequencing. A guide to the construction of plasmids used in this study is detailed in **Table S3**. The plasmid (pAL2244, **Table S1**) containing the linear fragment for the integration of the gene formate dehydrogenase from *Arabidopsis thaliana* (hereafter *At*) expressed under the Biobricks strong constitutive promoter $P_{BBa\_J23119}$ was integrated into safe site 9 (Bassalo et al., 2016) of *E. coli* using Clustered Regularly Interspaced Short Palindromic Repeats (CRISPR)/Cas9 (Jiang et al., 2015) and was codon optimized and purchased from Genewiz from Azenta Life Sciences.

**CRISPR**

Genome modifications such as gene deletion and gene insertion were constructed using CRISPR-Cas9-mediated homologous recombination (Jiang et al., 2015). Linear DNA repair fragments for gene deletions and insertions were constructed by amplifying genomic or plasmid DNA via PCR assembly (Xiong et al., 2004). Plasmids encoding sgRNA for CRISPR-Cas9-mediated homologous recombination were constructed using Q5 site-directed mutagenesis (New England Biolabs) using pTargetF plasmid (Addgene #62226) as a template. All genomic modifications were verified via Sanger Sequencing. A guide for CRISPR-Cas9-mediate gene deletions and insertions used in this study is detailed in **Table S4**.

**Culture Conditions**

Overnight cultures were prepared in 3 mL of Luria-Bertani (LB) media containing appropriate antibiotics. Antibiotic concentrations were as follows: tetracycline (5 μg $mL^{-1}$), spectinomycin (25 μg $mL^{-1}$), kanamycin (25 μg $mL^{-1}$), ampicillin (100 μg $mL^{-1}$). Low density isobutanol experiments were carried out in 5 mL M9P: M9 minimal media (33.7 mM $Na_2HPO_4$, 22 mM $KH_2PO_4$, 8.6 mM NaCl, 9.4 mM $NH_4Cl$, 1 mM $MgSO_4$, 0.1 mM $CaCl_2$) including A5 trace metal mix (2.86 mg $L^{-1}$ $H_3BO_3$, 1.81 mg $L^{-1}$ $MnCl_2{\cdot}4H_2O$, 0.079 mg $L^{-1}$ $CuSO_4{\cdot}5H_2O$, 49.4 μg $L^{-1}$ $Co(NO_3)_2{\cdot}6H_2O$) supplemented with 5 g $L^{-1}$ yeast extract (Research Products International) and 10 g $L^{-1}$ glucose (Fisher Bioreagents) with additional appropriate carbon sources. Overnight culture in LB media was spun down at 6,000 *g* for 1 min. The cell pellet was re-suspended with 5 mL M9P media. The M9P culture was grown to an $OD_{600}$ of ~0.4 and subsequently spun down at 6,000 *g* for 1 min. The pellet was resuspended in 5 mL M9P supplemented with appropriate carbon sources and was induced with 1 mM IPTG and 10 μg $L^{-1}$ aTc. Cultures were incubated at 37 °C. Cell growth was monitored by measuring $OD_{600}$ in a Synergy HTX Plate Reader (BioTek Instruments, Inc.).

For high density experiments, overnight culture was used to inoculate a 250 mL screw cap flask containing 50 mL M9P. The 50 mL culture was allowed to grow to an $OD_{600}$ of ~0.4 and was induced with 1 mM IPTG and 10 µg $L^{-1}$ aTc. The culture was allowed to grow for an additional 1.5 h to an $OD_{600}$ of ~1. The 50 mL culture was centrifuged at 6,000 *g* for 5 min and resuspended in 1 mL of M9P with appropriate carbon sources for an $OD_{600}$ of ~50.

**Preparation of Catalyst**

The catalyst $[Na(diglyme)_2][Fe_4N(CO)_{12}]$ was prepared according to a reported procedure (Noviandri et al., 1999).

**Electrochemical Measurements**

Cyclic voltammograms (CV's) were recorded under a $N_2$ or $CO_2$ gas ($N_2$) (99.998%, Praxair) atmosphere using an electrochemical analyzer (CH Instruments, Model 620D or Model 1100B), a glassy carbon working electrode (CH Instruments) with a nominal surface area of 0.0707 $cm^2$), and a platinum wire auxiliary electrode. Controlled electrode potential (CPE) experiment was performed on a multichannel Biologic VSP 300 potentiostat. The glassy carbon working electrode was polished on a felt pad with alumina paste (0.05 µm, BASi), sonicated in deionized water, rinsed with MeOH, and dried with a Kimwipe prior to each experiment. As the reference electrode, a Ag/AgCl(sat.) electrode was used form aqueous measurements. All reported potentials are referenced to the SCE couple, and were determined using ferrocene (Aldrich) as an internal standard, where $E_{1/2}$ ($Fc^{+1/0}$ ) is +0.159 V vs SCE in water (Noviandri et al., 1999). Milli-Q water (18 MΩ) was used for measurements performed in aqueous solution. Buffer solutions were 0.1 M phosphate buffer adjusted to pH 7.4. Reagents for buffer preparation were purchased from EMD, VWR, and Sigma, and were used as received. In all cases, CV sweeps were initiated at the open circuit potential and recorded in quiescent solution.

**Controlled Potential Electrolysis (CPE)**

CPE experiments were performed in a gas-tight glass cell (working electrode compartment volume of 60 mL) under 1 atm of static $N_2$ (Praxair, 99.998%) or carbon dioxide (Praxair, 99.5%) with a stirred solution. The cell was custom made by Adams & Chittenden Scientific glass (**Fig. S1**). The counter electrode compartment was separated from the working electrode compartment by a glass frit of medium porosity. In a typical experiment, 20 mL of degassed 0.1 M phosphate buffer solution (made from 0.05 M $Na_2HPO_4$/0.05 M $NaH_2PO_4$ was used in the working electrode compartment along with 0.5 mM $Na(diglyme)_2[Fe_4N(CO)_{12}]$ (diglyme: bis(2-methoxyethyl) ether). In control experiments performed with the same solutions absent the iron catalyst no formate was detected, only ~ 2 C of charge were passed over 1 h and low levels of $H_2$ were detected, consistent with our prior reports (Taheri et al., 2015).

The working electrode was a glassy carbon plate with an area of 8 $cm^2$ (Tokai Carbon), while the counter electrode was a coiled Pt wire ~70 cm in length (0.5 mm diameter, 99.997% metals basis from Alfa aesar). The reference electrodes employed for CPE experiments were of

similar design to those used for CV measurements, using a longer glass tube to fit the H-cell. Between CPE experiments, the glass cell, the stir bar, the working electrode, and the counter electrode were cleaned via sonication in 5% (v/v) nitric acid for 5 min, rinsed with deionized (DI) water, sonicated in DI water for 5 min, rinsed with DI water, and then sonicated in acetone for 5 min, rinsed with DI water, and allowed to dry in an oven before use. Every two weeks the frit was checked and baked out or changed by a glassblower. The glassy carbon plate had an additional initial step of being thoroughly sanded on all surfaces with 300 grit SiC paper and then 600 grit SiC paper and rinsed with water prior to sonication steps. The counter electrode (Pt coil) was flame annealed prior to each experiment. For longer CPE runs (more than 20 h) both the cathodic and anodic compartment was purged with humidified $CO_2$ in each hour and the anode chamber was purged with N2 gas. A home-built intermittent purging valve set up was used for purging. During CPE the pH of the solution was monitored by a Bluelab pH controller (Bluelab USA). In those longer CPE experiments no headspace measurements were performed to detect $H_2$ gas. Faradaic Efficiency (FE) was determined by calculating the amount of charge required in production of each product divided by total charge passed during each experiment.

Quantification of headspace gases and solution-phase products were performed separately (Taheri et al., 2015). At the end of an electrolysis, a gaseous sample (0.1 mL) was drawn from the headspace, using a gas-tight syringe (Vici), and injected into a gas chromatography−thermal conductivity detection (GC- TCD) system (Model Varian 3800 GC coupled with a TCD detector and a Carboxen 1010 PLOT fused silica column (30 m × 0.53 mm) (Supelco) using N2 (99.999%, Praxair) as the carrier gas. $H_2$ concentration was determined using a previously prepared working curve (Taheri et al., 2015). Analysis of the liquid phase and determination of formate content was achieved by removing 0.5 mL of sample from the CPE experiment and analyzed via high performance liquid chromatography described below.

**Bio-electrochemical cultivation for isobutanol production**

Following the CPE experiment, a syringe was used to remove 20 mL of solution from the working electrode side of the cell. The CPE solution was supplemented with 50 mM sodium bicarbonate and 10 g $L^{-1}$ glucose. Antibiotics and inducers (IPTG and aTc) were also added in appropriate amounts. Overnight cultures were prepared in 3 mL of Luria-Bertani (LB) media containing appropriate antibiotics. Overnight LB culture was used to inoculate a 250 mL screw cap culture flask containing 50 mL M9P. The culture was grown to an $OD_{600}$ of 0.4 and induced with IPTG and aTc. The culture was allowed to grow for an additional 1.5 hours to an $OD_{600}$ of approximately 1. The culture was then centrifuged at 6,000 *g* for 5 minutes. The cell pellet was resuspended in 1 mL of the solution made using the reaction mixture following the CPE experiment. 100 µL was removed from the bacterial culture are regular intervals and subsequently analyzed using Gas chromatography (GC) and High Performance Liquid Chromatography (HPLC).

**GC analysis**

Concentrations of isobutanol were analyzed by GC–FID. The GC system is a GC-2010 with an AOC-20 S auto sampler and AOC-20i auto injector (Shimadzu). The column used was a DB-WAX capillary column (30 m length, 0.32 mm diameter and 0.5 µm film thickness; Agilent Technologies). The GC oven temperature was held at 225 °C, and the FID was held at 330 °C. The injection volume was 0.5 µl, injected at a 15:1 split ratio. Helium was used as the carrier gas. Retention times from samples were compared with standards.

To prepare samples for GC analysis, 1 ml of cell culture was centrifuged at 20,000 *g* for 10 min at 25 °C. 100 µL of culture supernatant was diluted with 900 µL MilliQ water.

**HPLC analysis**

Concentrations of glucose and formate were analyzed by 20A HPLC (Shimadzu) equipped with a differential refractive detector 10A and an Aminex fast acid analysis column (Bio-Rad). The mobile phase was 5 mM of $H_2SO_4$, maintained at a flow rate of 0.6 ml $min^{-1}$ at 65 °C for 12.5 min.

To prepare bacterial samples for HPLC analysis, 1 mL of cell culture was centrifuged at 20,000 g for 10 min at 25°C. 10 µL of filtered culture supernatant or of the liquid phase from CPE experiments was injected into the column for analysis.

**Stable isotype tracer analysis**

To prepare samples for metabolomics analysis, 0.5 mL of cell cultures were frozen in liquid nitrogen and stored at -80°C until analysis. Metabolite extraction, derivatization and analysis by GC-TOF-MS was carried out by the West Coast Metabolomics Center at University of California, Davis.

## Results and Discussion

### Isobutanol Production in Reductive Glycine Pathway Strain

In the previous study, the RGP was constructed in the *E. coli* strain, YT151 (Strain 1, **Table 1**) (Tashiro et al., 2018). The RGP containing a formate assimilation pathway constructed from three genes from *Clostridium ljungdahlii* (Köpke et al., 2010) (hereafter *Cl*): a formate-tetrahydrofolate ligase encoded by *fhs* (Paukert and Rabinowitz, 1980), methenyl-THF cyclohydrolase encoded by *fchA* (Clark and Ljungdahl, 1982), and methylene-THF dehydrogenase encoded by *folD* (Suarez de Mata and Rabinowitz, 1980) was combined with the expression of the glycine cleavage system in the reverse direction (rGCS) (Kikuchi et al., 2008; Tashiro et al., 2018) (pYT100, **Table S1**). The RGP was shown to function in *E. coli*; metabolomics data from this study showed that labelled formate and $CO_2$ were assimilated into L-alanine via pyruvate (Tashiro et al., 2018). The isobutanol production plasmid (pAL603, **Table S1**) (Desai et al., 2014) was introduced to Strain 1 to determine if isobutanol production could be aided by Strain 1's ability to assimilate C1 substrates into central metabolism. The isobutanol production pathway was constructed from five genes: an acetolactate synthase from *Bacillus subtilis* encoded by *alsS* (Gollop et al., 1990), a ketol-acid reductoisomerase and a dihydroxy-

acid dehydratase from *E. coli* encoded by *ilvC* and *ilvD* (Atsumi et al., 2008b), respectively, a ketoacid decarboxylase from *Lactococcus lactis* encoded by *kivD* (De La Plaza et al., 2004), and an alcohol dehydrogenase from *Lactococcus lactis* encoded by *adhA* (Bolotin et al., 2001). This isobutanol pathway was shown to be efficient at converting pyruvate into isobutanol in previous studies (Atsumi et al., 2008b; Desai et al., 2014). The production of isobutanol with and without the RGP plasmids (pYT100 and pAL2236, **Table S1**) was compared in M9P with 50 mM $NaHCO_3$ and 0.2 g $L^{-1}$ formate. Strain 1 with the RGP was not able to produce isobutanol, while Strain 1 without the RGP produced 1.75 g $L^{-1}$ isobutanol in 48 h (**Fig. S2a**). The results suggested that there is metabolic imbalance preventing the synthesis of isobutanol. We hypothesized that intracellular NADH/NADPH levels were not sufficient to provide the energetic requirements for both pathways. Thus, the gene encoding for $NADP^+$-dependent formate dehydrogenase (Fdh) from *At* (Bang et al., 2020) was integrated into safe site 9 (SS9) (Bassalo et al., 2016) in the chromosome of Strain 1, generating Strain 2 (**Table 1**). Strain 2 with the isobutanol production and the RGP plasmids was able to produce isobutanol at 2.23 g $L^{-1}$, suggesting that additional reducing equivalents are required to produce isobutanol with the RGP. These three strains produced formate in the first day and consumed formate slightly in the second day (**Fig. S2b**). The results suggested inefficiency in the formate assimilation of the strains.

**Engineering Isobutanol Strain with Reductive Glycine Pathway**

To improve isobutanol production, this system was moved into AL17 which was designed for isobutanol production (Strain 3, **Table 1**) (Atsumi et al., 2008b). This strain possesses several gene deletions that were generated to direct flux away from other fermentation products (Atsumi et al., 2008b, 2008a). Particularly, the deletion of *pflB*, which encodes for a pyruvate formate-lyase eliminated formate production in Strain 3 (Atsumi et al., 2008a). The deletion of *pflB* was also used to improve the pyruvate forming flux from formate and $CO_2$ of an *E. coli* strain by preventing the production of formate from intracellular pyruvate (Bang et al., 2020). Notably, Strain 3 harboring the isobutanol production and the RGP plasmids was able to produce 3.19 g $L^{-1}$ isobutanol without the addition of Fdh indicating that the genomic modifications present in AL17 allow for more efficient production of isobutanol (**Fig. 2a**). Strain 3 consumed formate, indicating that the formate assimilation inefficiencies present in earlier strains (**Fig. S2b**) were overcome in this strain. In Strain 3, L-serine can be produced by the RGP and the native L-serine biosynthetic pathway. We hypothesized that the L-serine produced from the native biosynthetic pathway decreases the efficiency of the RGP by inhibiting flux through the RGP due to the accumulation of L-serine as a product which would shift equilibrium to favor the reverse of the desired reaction back towards formate and $CO_2$, according to Le Châtelier's principle. The *serA* gene was deleted from the chromosome of Strain 3, generating Strain 4 (**Table 1**). The titer and the yield of isobutanol production were improved in Strain 4 compared to Strain 3 (**Fig. 2a**), suggesting that the carbon being assimilated by the RGP is more efficient in aiding the production of isobutanol when glucose metabolism is cut off

from L-serine synthesis. This result could be due to flux, by necessity, increasing towards L-serine from formate and $CO_2$ when serine is unable to be synthesized from glucose.

**Formate Dehydrogenase Screening**

The expression of *fdh* (*At*) improved isobutanol production (**Fig. S2a**). We screened two other variants of formate dehydrogenase to determine if there was a similar benefit to either production or yield. The Fdhs from *Candida boidinii* (hereafter *Cb*) and *Saccharomyces cerevisiae* (hereafter *Sc*) are $NAD^+$-dependent (Guo et al., 2016; Overkamp et al., 2002), while Fdh (*At*) is $NADP^+$-dependent. Each Fdh variant has been previously shown to enhance reducing equivalent pools in *E. coli,* which we hypothesized would improve isobutanol production in our strain (Bang et al., 2020; Calzadiaz-Ramirez et al., 2020; Shen et al., 2011; Wang et al., 2013). The corresponding gene was cloned under the constitutive promoter $P_{BBa\_J23119}$ and integrated into SS9 (Jeong et al., 2012)), generating Strains 5 (*At*), 6 (*Cb*), and 7 (*Sc*) (**Table 1**). Strain 6 consumed the most formate and produced isobutanol with the best yield of the three strains (**Fig. 2b**). Although Strain 7 produced more isobutanol than Strain 6, the yield was the worst of the three strains (**Fig. 2b**). Thus, we proceeded with Strain 6 for future experiments.

**Strain and Fermentation Optimization**

It has been shown that replacing the native promoter of *sdaA* ($P_{sdaA}$) to $P_{LlacO1}$ (Lutz and Bujard, 1997) enhanced the conversion of formate and $CO_2$ to pyruvate in the RGP (Tashiro et al., 2018). The gene *sdaA* encodes for an endogenous L-serine deaminase which catalyzes the conversion of L-serine to pyruvate and was previously determined to be the optimal target for overexpression to enhance growth on L-serine (Tashiro et al., 2018). To test if the promoter replacement improves isobutanol production, $P_{sdaA}$ was replaced with $P_{LlacO1}$ in Strain 6, generating Strain 8 (**Table 1**). This modification improved the yield (**Fig. S3**), demonstrating that more carbon from the RGP was being incorporated into isobutanol.

To reduce the impact of cell growth on isobutanol production, a high density (Optical Density at 600 nm ($OD_{600}$) > 30) was conducted to elucidate the ability of the engineered strain to act as a whole cell non-growing biocatalyst (Shiloach and Fass, 2005), capable of converting RGP substrates into isobutanol. In this experiment an induced culture of the strains was grown to an approximate $OD_{600}$ of 1 and subsequently centrifuged and resuspended in 1/50th the volume of fresh experimental media generating a dense non-growing slurry of *E. coli*. Strains 4, 6 and 8 were compared to elucidate the effects of expressing both *fdh* and *sdaA* on isobutanol production. Strains 6 and 8 produced 3.48 and 3.35 g $L^{-1}$ isobutanol respectively, showing that a non-growing biocatalytic expression system is beneficial for overall chemical production (**Fig. 2c**). Strain 8 performed the best with respect to yield, achieving a yield of 0.43 g isobutanol per g glucose (g $g^{-1}$) which is 101% of the theoretical max yield of isobutanol produced from glucose alone (0.41 g $g^{-1}$). Theoretical maximum yield was calculated by determining a maximum of one mole of isobutanol can be produced per mole of glucose consumed. Achieving above 100% of theoretical maximum yield indicates that the genomic modifications in this strain facilitate the incorporation of formate and $CO_2$ into isobutanol. An additional experiment was carried out

under identical methodology where Strain 8 was cultivated with and without formate and bicarbonate (**Fig. 3**). Without formate and/or bicarbonate present in the media resulted in lower yield when compared to the condition where both bicarbonate and formate were present, indicating that formate and bicarbonate aid in the production of isobutanol in this strain (**Fig. 3**).

A stable isotype tracer analysis was performed to ensure that the single carbon substrates were indeed incorporated into central metabolism and into the isobutanol production pathway wherein $^{13}$C-labeled formate and bicarbonate were fed to Strain 8 under low density conditions. The carbon at position 1 and position 2 in glycine came from $CO_2$ and formate, respectively (**Fig. 4**) (Kikuchi et al., 2008). When unlabeled bicarbonate and formate were used, there was no enrichment of M1 and M2 with relative abundance of these ions matching data from the NIST library standards (**Fig. 4**). When labeled bicarbonate and formate were used, the M1 and M2 were twice as abundant, indicating that the RGP is functioning as intended (**Fig. 4**). The intermediate 2-ketoisovalerate was also analyzed using this stable isotope tracer analysis and it was determined that M1 was enriched by 4.3%, indicating that some of the formate and bicarbonate is flowing through the RGP towards isobutanol. Since the RGP connects to pyruvate much of the labeled formate and bicarbonate is likely flowing to other metabolites unrelated to isobutanol production and further study is required to mitigate this flux away from the product of interest.

To further demonstrate the ability of this engineered strain to leverage formate and $CO_2$ to produce isobutanol an additional high-density experiment was carried out wherein the only carbon sources were formate and $CO_2$. Isobutanol production was observed, suggesting that the engineered strain can integrate single carbon substrates into isobutanol (**Fig. S4**).

**Coupling Electrocatalysis with Engineered Strain**

A series of controlled potential electrolysis (CPE) experiments were performed using the catalyst $[Na(diglyme)_2][Fe_4N(CO)_{12}]$ (**Table 2, Fig. S1**). The applied potential was selected by performing a series of CPE experiments over the applied potential range of −1.12 - −1.24 V to determine where formate production rate and selectivity over $H_2$ production would be highest (**Fig. S5**). A potential of −1.2 V was selected based on those experiments which were run over 1 h each. For production of formate to support isobutanol production the CPE experiments were run over 20 h and the cathode chamber was purged every 1 h with humidified $CO_2$. Control blank CPE experiments with no added catalyst show significantly lower amounts of charge passed during 20 h CPE experiment (**Table 2**). We also ran a CPE experiment with the used glassy carbon working electrode (rinse test) to ensure that deposition of catalyst or other materials was not responsible for the catalysis: no formate was detected from that experiment. The stability and homogeneous nature of the catalyst was tested before and after CPE experiments by recording infrared spectra of CPE solution to make sure that the catalyst is still present in solution. Peaks characteristic of $[Na(diglyme)_2][Fe_4N(CO)_{12}]$ were observed at 2015

and 1989 $cm^{-1}$ and were present before and after CPE experiments indicating that the catalyst was intact for each trial (**Fig. S6**).

In CPE experiments, 4.2 g $L^{-1}$ formate was produced after 21 hours using 0.5 mM catalyst (**Table 2**) which demonstrates the ability of this catalyst to convert $CO_2$ efficiently into formate. This formate production rate of 0.2 g $L^{-1}$ $h^{-1}$ is relatively slow compared with published work (Fernández-Caso et al., 2023) that employs gas diffusion electrodes and heterogeneous electrocatalysts such as tin, bismuth, or lead and operate at > 10 g $L^{-1}$ $h^{-1}$. However, here we have used a traditional H-cell set up which has slow diffusion kinetics and low solubility of $CO_2$ in the aqueous buffer, and this choice of the electrochemical cell could be modified in future work to access faster formate production rates (Alinejad et al., 2022; Hernandez-Aldave and Andreoli, 2020). Formate is the most readily synthesized chemical from $CO_2$ using electrocatalytic methods (Taheri et al., 2015). The use of an Earth-abundant material such as iron that can continue to produce formate for long periods (> 20 h) also represents one of the more renewable and sustainable methodologies to sequester carbon. To demonstrate the electrocatalytically produced formate could be upcycled into other valuable chemicals, we cultivated Strain 8 using the CPE reaction mixture, supplemented with 50 mM $NaHCO_3$ and 10 g $L^{-1}$ glucose (**Fig. 5**). The engineered *E. coli* consumed the formate produced electrocatalytically at a rate of 1.84 g $L^{-1}$ $h^{-1}$ (**Fig. 5b**) under high density conditions during the production of isobutanol without the need to purify formate away from the reaction mixture. Strain 8 could produce isobutanol with a high productivity (2.53 g $L^{-1}$ $h^{-1}$) using an electrocatalytic reaction mixture (**Fig. 5c**). This is in contrast to other hybrid systems reported where the produced compound must be purified away from toxic compounds prior to being used as a substrate for an engineered microorganism (Orella et al., 2020; Zheng et al., 2022). This finding demonstrates that efficient electrocatalytic reduction of $CO_2$ can be coupled to biochemical production to convert formate into the valuable chemical commodity isobutanol. This study represents a significant advance towards sustainably producing chemicals from $CO_2$.

## Conclusion

Here we have shown that a non-RuBisCO based $CO_2$ fixation method, the RGP, can be efficiently used to bolster the production of a value-added chemical commodity. By creating a hybrid system, we can link renewable sources of electricity with the production of an energy dense chemical commodity. This electrical-biological hybrid system has several benefits over electrochemical or biological production alone. The production of formate from $CO_2$ by electrochemical methods has established a more rapid method of carbon sequestration than carbon capture by photosynthesis. The use of formate as a feedstock for *E. coli* has led to an efficient electrocatalysis platform for the production of isobutanol, a stable, high-energy and valuable chemical.

The RGP is a promising platform for $CO_2$ assimilation in microbes. Additionally, there are several reasons that both *E. coli* and the RGP are promising candidates for future optimization of a hybrid electrical-biological system for $CO_2$ fixation. First, *E. coli* has been shown to be a

viable host for the RGP that requires minimal metabolic perturbations in order to establish a $CO_2$ fixing strain. Second, two-thirds of the carbons in the RGP come from formate, which can be readily synthesized in an electrocatalytic setting. Third, *E. coli* is a well-established host organism, allowing us to balance various parameters of metabolism and generate metabolic changes quickly as was done when screening and installing formate dehydrogenase.

As renewable sources of energy production become more widespread, a surplus of electricity is generated during the day, resulting in excess unused energy. By using this excess to electrocatalytically capture $CO_2$ we can improve the environmental impact of renewable energy generation. By combining electrocatalytic systems with microbial production platforms, we can link efficient carbon capture methods with the bio-based production of valuable chemical commodities. Additionally, by showing that *E. coli* can incorporate electrocatalytically produced formate that was generated using a more efficient catalyst into central metabolism, we have shown that as these fields continue to grow, advances in either field can add an overall benefit to the sustainability and efficiency of hybrid systems.

## Data availability

The datasets generated in this study are available from the corresponding author on reasonable request.

## References


Alinejad, S., Quinson, J., Wiberg, G.K.H., Schlegel, N., Zhang, D., Li, Y., Reichenberger, S., Barcikowski, S., Arenz, M., 2022. Electrochemical Reduction of $CO_2$ on Au Electrocatalysts in a Zero-Gap, Half-Cell Gas Diffusion Electrode Setup: a Systematic Performance Evaluation and Comparison to an H-cell Setup**. ChemElectroChem 9, 1–11. https://doi.org/10.1002/celc.202200341

Atsumi, S., Cann, A.F., Connor, M.R., Shen, C.R., Smith, K.M., Brynildsen, M.P., Chou, K.J.Y., Hanai, T., Liao, J.C., 2008a. Metabolic engineering of *Escherichia coli* for 1-butanol production. Metab. Eng. 10, 305–311. https://doi.org/10.1016/j.ymben.2007.08.003

Atsumi, S., Hanai, T., Liao, J.C., 2008b. Non-fermentative pathways for synthesis of branched-chain higher alcohols as biofuels. Nature 451, 86–89. https://doi.org/10.1038/nature06450

Bang, J., Hwang, C.H., Ahn, J.H., Lee, J.A., Lee, S.Y., 2020. *Escherichia coli* is engineered to grow on $CO_2$ and formic acid. Nat. Microbiol. 5, 1459–1463. https://doi.org/10.1038/s41564-020-00793-9

Barecka, M.H., Ager, J.W., Lapkin, A.A., 2021. Carbon neutral manufacturing via on-site $CO_2$ recycling. iScience 24, 102514. https://doi.org/10.1016/j.isci.2021.102514

Bassalo, M.C., Garst, A.D., Halweg-Edwards, A.L., Grau, W.C., Domaille, D.W., Mutalik, V.K., Arkin, A.P., Gill, R.T., 2016. Rapid and Efficient One-Step Metabolic Pathway Integration in *E. coli*. ACS Synth. Biol. 5, 561–568. https://doi.org/10.1021/acssynbio.5b00187

Bolotin, A., Wincker, P., Mauger, S., Jaillon, O., Malarme, K., Weissenbach, J., Ehrlich, S.D., Sorokin, A., 2001. The Complete Genome Sequence of the Lactic Acid Bacterium *Lactococcus lactis* ssp. lactis IL1403 . Genome Res. 11, 731–753. https://doi.org/10.1101/gr.169701

Calzadiaz-Ramirez, L., Calvó-Tusell, C., Stoffel, G.M.M., Lindner, S.N., Osuna, S., Erb, T.J., Garcia-Borràs, M., Bar-Even, A., Acevedo-Rocha, C.G., 2020. *In Vivo* Selection for Formate Dehydrogenases with High Efficiency and Specificity toward $NADP^+$. ACS Catal. 10, 7512–7525. https://doi.org/10.1021/acscatal.0c01487

Case, A.E., Atsumi, S., 2016. Cyanobacterial chemical production. J. Biotechnol. 231, 106–114. https://doi.org/10.1016/j.jbiotec.2016.05.023

Chen, H., Dong, F., Minteer, S.D., 2020. The progress and outlook of bioelectrocatalysis for the production of chemicals, fuels and materials. Nat. Catal. 3, 225–244. https://doi.org/10.1038/s41929-019-0408-2

Chen, L., Msigwa, G., Yang, M., Osman, A.I., Fawzy, S., Rooney, D.W., Yap, P.S., 2022. Strategies to achieve a carbon neutral society: a review, Environmental Chemistry Letters. Springer International Publishing. https://doi.org/10.1007/s10311-022-01435-8

Cheng, M.-H., Huang, H., Dien, B.S., Singh, V., 2019. The costs of sugar production from different feedstocks and processing technologies. Biofuel Bioprod Biorefin 13, 723–739. https://doi.org/https://doi.org/10.1002/bbb.1976

Clark, J., Ljungdahl, L.G., 1982. Purification and properties of 5,10-methenyltetrahydrofolate cyclohydrolase from *Clostridium formicoaceticum*. J Biol Chem 257, 3833–3836. https://doi.org/10.1016/s0021-9258(18)34857-9

De La Plaza, M., Fernández De Palencia, P., Peláez, C., Requena, T., 2004. Biochemical and molecular characterization of α-ketoisovalerate decarboxylase, an enzyme involved in the formation of aldehydes from amino acids by *Lactococcus lactis*. FEMS Microbiol. Lett. 238, 367–374. https://doi.org/10.1016/j.femsle.2004.07.057

Desai, S.H., Rabinovitch-Deere, C.A., Tashiro, Y., Atsumi, S., 2014. Isobutanol production from cellobiose in *Escherichia coli*. Appl. Microbiol. Biotechnol. 98, 3727–3736. https://doi.org/10.1007/s00253-013-5504-7

Döring, V., Darii, E., Yishai, O., Bar-Even, A., Bouzon, M., 2018. Implementation of a Reductive Route of One-Carbon Assimilation in *Escherichia coli* through Directed Evolution. ACS Synth. Biol. 7, 2029–2036. https://doi.org/10.1021/acssynbio.8b00167

Fernández-Caso, K., Díaz-Sainz, G., Alvarez-Guerra, M., Irabien, A., 2023. Electroreduction of CO2: Advances in the Continuous Production of Formic Acid and Formate. ACS Energy Lett. 8, 1992–2024. https://doi.org/10.1021/acsenergylett.3c00489

Geleynse, S., Brandt, K., Garcia-Perez, M., Wolcott, M., Zhang, X., 2018. The Alcohol-to-Jet Conversion Pathway for Drop-In Biofuels: Techno-Economic Evaluation. ChemSusChem 11, 3728–3741. https://doi.org/10.1002/cssc.201801690

Goeppert, A., Czaun, M., Jones, J.P., Surya Prakash, G.K., Olah, G.A., 2014. Recycling of carbon dioxide to methanol and derived products-closing the loop. Chem. Soc. Rev. 43, 7995–8048. https://doi.org/10.1039/c4cs00122b

Gollop, N., Damri, B., Chipman, D.M., Barak, Z., 1990. Physiological implications of the substrate specificities of acetohydroxy acid synthases from varied organisms. J. Bacteriol. 172, 3444–3449. https://doi.org/10.1128/jb.172.6.3444-3449.1990

Guo, Q., Gakhar, L., Wickersham, K., Francis, K., Vardi-Kilshtain, A., Major, D.T., Cheatum, C.M., Kohen, A., 2016. Structural and Kinetic Studies of Formate Dehydrogenase from *Candida boidinii*. Biochemistry 55, 2760–2771. https://doi.org/10.1021/acs.biochem.6b00181

Hernandez-Aldave, S., Andreoli, E., 2020. Fundamentals of gas diffusion electrodes and electrolysers for carbon dioxide utilisation: Challenges and opportunities. Catalysts. https://doi.org/10.3390/CATAL10060713

Jeong, J.Y., Yim, H.S., Ryu, J.Y., Lee, H.S., Lee, J.H., Seen, D.S., Kang, S.G., 2012. One-step sequence-and ligation-independent cloning as a rapid and versatile cloning method for functional genomics Studies. Appl. Environ. Microbiol. 78, 5440–5443. https://doi.org/10.1128/AEM.00844-12

Jiang, Y., Chen, B., Duan, C., Sun, B., Yang, J., Yang, S., 2015. Multigene editing in the *Escherichia coli* genome via the CRISPR-Cas9 system. Appl. Environ. Microbiol. 81, 2506–2514. https://doi.org/10.1128/AEM.04023-14

Kikuchi, G., Motokawa, Y., Yoshida, T., Hiraga, K., 2008. Glycine cleavage system. Proc. Natl. Acad. Sci. U. S. A. 84, 246–263. https://doi.org/10.2183/pjab/84.246

Köpke, M., Held, C., Hujer, S., Liesegang, H., Wiezer, A., Wollherr, A., Ehrenreich, A., Liebl, W., Gottschalk, G., Dürre, P., 2010. *Clostridium ljungdahlii* represents a microbial production platform based on syngas. Proc. Natl. Acad. Sci. U. S. A. 107, 13087–13092. https://doi.org/10.1073/pnas.1004716107

Li, H., Opgenorth, P.H., Wernick, D.G., Rogers, S., Wu, T.Y., Higashide, W., Malati, P., Huo, Y.X., Cho, K.M., Liao, J.C., 2012. Integrated electromicrobial conversion of $CO_2$ to higher alcohols. Science. 335, 1596. https://doi.org/10.1126/science.1217643

Lim, J., Choi, S.Y., Lee, J.W., Lee, S.Y., Lee, H., 2023. Biohybrid $CO_2$ electrolysis for the direct synthesis of polyesters from $CO_2$. Proc. Natl. Acad. Sci. 120, e2221438120. https://doi.org/10.1073/pnas.2221438120

Loewen, N.D., Neelakantan, T. V, Berben, L.A., 2017. Renewable Formate from C-H Bond Formation with $CO_2$: Using Iron Carbonyl Clusters as Electrocatalysts. Acc. Chem. Res. 50, 2362–2370. https://doi.org/10.1021/acs.accounts.7b00302

Lutz, R., Bujard, H., 1997. Independent and tight regulation of transcriptional units in escherichia coli via the LacR/O, the TetR/O and AraC/I1-I2 regulatory elements. Nucleic Acids Res. 25, 1203–1210. https://doi.org/10.1093/nar/25.6.1203

Lynd, L.R., Cushman, J.H., Nichols, R.J., Wyman, C.E., 1991. Fuel Ethanol from Cellulosic Biomass. Science. 251, 1318–1323. https://doi.org/10.1126/science.251.4999.1318

Nitopi, S., Bertheussen, E., Scott, S.B., Liu, X., Engstfeld, A.K., Horch, S., Seger, B., Stephens, I.E.L., Chan, K., Hahn, C., Nørskov, J.K., Jaramillo, T.F., Chorkendorff, I., 2019. Progress and Perspectives of Electrochemical $CO_2$ Reduction on Copper in Aqueous Electrolyte. Chem. Rev. 119, 7610–7672. https://doi.org/10.1021/acs.chemrev.8b00705

Noviandri, I., Brown, K.N., Fleming, D.S., Gulyas, P.T., Lay, P.A., Masters, A.F., Phillips, L., 1999. The Decamethylferrocenium/Decamethylferrocene Redox Couple: A Superior Redox Standard to the Ferrocenium/Ferrocene Redox Couple for Studying Solvent Effects on the Thermodynamics of Electron Transfer. J. Phys. Chem. B 103, 6713–6722. https://doi.org/10.1021/jp991381+

Orella, M.J., Brown, S.M., Leonard, M.E., Román-Leshkov, Y., Brushett, F.R., 2020. A General Technoeconomic Model for Evaluating Emerging Electrolytic Processes. Energy Technol. 8, 1–12. https://doi.org/10.1002/ente.201900994

Overkamp, K.M., Ktter, P., Van Hoek, R. Der, Schoondermark-Stolk, S., Luttik, M.A.H., Van Dijken, J.P., Pronk, J.T., 2002. Functional analysis of structural genes for $NAD^+$ -dependent formate dehydrogenase in *Saccharomyces cerevisiae*. Yeast 19, 509–520. https://doi.org/10.1002/yea.856

Paukert, J.L., Rabinowitz, J.C., 1980. [85] Formyl-Methenyl-Methylenetetrahydrofolate Synthetase (Combined): A Multifunctional Protein in Eukaryotic Folate Metabolism. Methods Enzymol. 66, 616–626. https://doi.org/10.1016/0076-6879(80)66515-X

Shen, C.R., Lan, E.I., Dekishima, Y., Baez, A., Cho, K.M., Liao, J.C., 2011. Driving forces enable high-titer anaerobic 1-butanol synthesis in Escherichia coli. Appl. Environ. Microbiol. 77, 2905–2915. https://doi.org/10.1128/AEM.03034-10

Shiloach, J., Fass, R., 2005. Growing *E. coli* to high cell density - A historical perspective on method development. Biotechnol. Adv. 23, 345–357. https://doi.org/10.1016/j.biotechadv.2005.04.004

Suarez de Mata, Z., Rabinowitz, J.C., 1980. Formyl-methenyl-methylenetetrahydrofolate synthetase(combined) from yeast. Biochemical characterization of the protein from an ADE3 mutant lacking the formyltetrahydrofolate synthetase function. J Biol Chem 255, 2569–2577. https://doi.org/10.1016/s0021-9258(19)85930-6

Taheri, A., Thompson, E.J., Fettinger, J.C., Berben, L.A., 2015. An Iron Electrocatalyst for Selective Reduction of $CO_2$ to Formate in Water: Including Thermochemical Insights. ACS Catal. 5, 7140–7151. https://doi.org/10.1021/acscatal.5b01708

Tashiro, Y., Hirano, S., Matson, M.M., Atsumi, S., Kondo, A., 2018. Electrical-biological hybrid system for $CO_2$ reduction. Metab. Eng. 47, 211–218. https://doi.org/10.1016/j.ymben.2018.03.015

Volanti, M., Cespi, D., Passarini, F., Neri, E., Cavani, F., Mizsey, P., Fozer, D., 2019. Terephthalic

acid from renewable sources: Early-stage sustainability analysis of a bio-PET precursor. Green Chem. 21, 885–896. https://doi.org/10.1039/c8gc03666g

Wang, W.C., Tao, L., 2016. Bio-jet fuel conversion technologies. Renew Sustain Energy Rev 53, 801–822. https://doi.org/10.1016/j.rser.2015.09.016

Wang, Y., Li, L., Ma, C., Gao, C., Tao, F., Xu, P., 2013. Engineering of cofactor regeneration enhances (2S,3S)-2,3-butanediol production from diacetyl. Sci. Rep. 3, 2643. https://doi.org/10.1038/srep02643

Xiong, A.S., Yao, Q.H., Peng, R.H., Li, X., Fan, H.Q., Cheng, Z.M., Li, Y., 2004. A simple, rapid, high-fidelity and cost-effective PCR-based two-step DNA synthesis method for long gene sequences. Nucleic Acids Res. 32, e98. https://doi.org/10.1093/nar/gnh094

Zheng, T., Zhang, M., Wu, L., Guo, S., Liu, X., Zhao, J., Xue, W., Li, J., Liu, C., Li, X., Jiang, Q., Bao, J., Zeng, J., Yu, T., Xia, C., 2022. Upcycling CO2 into energy-rich long-chain compounds via electrochemical and metabolic engineering. Nat. Catal. 5, 388–396. https://doi.org/10.1038/s41929-022-00775-6

**Acknowledgements**

This work was supported by University of California Carbon Neutrality Initiative and DOE ARPA-E (DE-AR0001513).

**Author contributions**

T.T, S.R., M.M., L.B, and S.A. designed research; T.T., S.P., M.C., and M.M. performed the experiments; T.T., S.P., L.B., and S.A. analyzed data; T.T., S.P, L.B., and S.A. wrote the manuscript.

**Competing interests**

The authors declare no competing interests.

592 **Table 1. List of key strains used in this study**

| Strain no. | Name | Key genotype | Ref |
|---|---|---|---|
| 1 | YT151 | BW25113/F'[*traD36*, *proAB*+, *lacI*$^q$ *Z*ΔM15 *Tn*10(Tet$^R$)] Δ*serA* | (Tashiro et al., 2018) |
| 2 | AL4068 | 1 + SS9::$P_{BBa\_J23119}$:*fdh* (*At*) | This work |
| 3 | AL17 | BW25113/F'[*traD36*, *proAB*$^+$, *lacI*$^q$ *Z*ΔM15 *Tn*10(Tet$^R$)] Δ*adhE* Δ*frdBC* Δ*fnr-ldhA* Δ*pta* Δ*pflB* | (Atsumi et al., 2008b) |
| 4 | AL4014 | 3 + Δ*serA* | This work |
| 5 | AL4101 | 4 + SS9::$P_{BBa\_J23119}$:*fdh* (*At*) | This work |
| 6 | AL4159 | 4 + SS9::$P_{BBa\_J23119}$:*fdh* (*Cb*) | This work |
| 7 | AL4160 | 4 + SS9::$P_{BBa\_J23119}$:*fdh* (*Sc*) | This work |
| 8 | AL4214 | 6 + $P_{sdaA}$::$P_{LlacO1}$ | This work |

593

594 **Table 2. CPE results for control experiments and experiments with catalyst**

| Experiments | Time/h | Charge (C) | FE(%) | Formate Yield (g L$^{-1}$) |
|---|---|---|---|---|
| Blank (No Catalyst) | 22 | 160 | 67% ($H_2$) | Not detected |
| 0.5 mM Catalyst | 22 | 354 | 84(5) ($HCOO^-$) | 4.2 (0.3) |
| Rinse test | 22 | 180 | 60% ($H_2$) | Not detected |

Applied potential ($E_{app}$) for CPEs is -1.2 V vs SCE, Detection limit of formate by HPLC is 0.05 g L$^{-1}$, FE is Faradic Efficiencies for $H_2$ and Formate. High FE for $H_2$ in blank and rinse test are the result of the ability of buffering anions to donate hydrogen directly to the electrode surface.

595

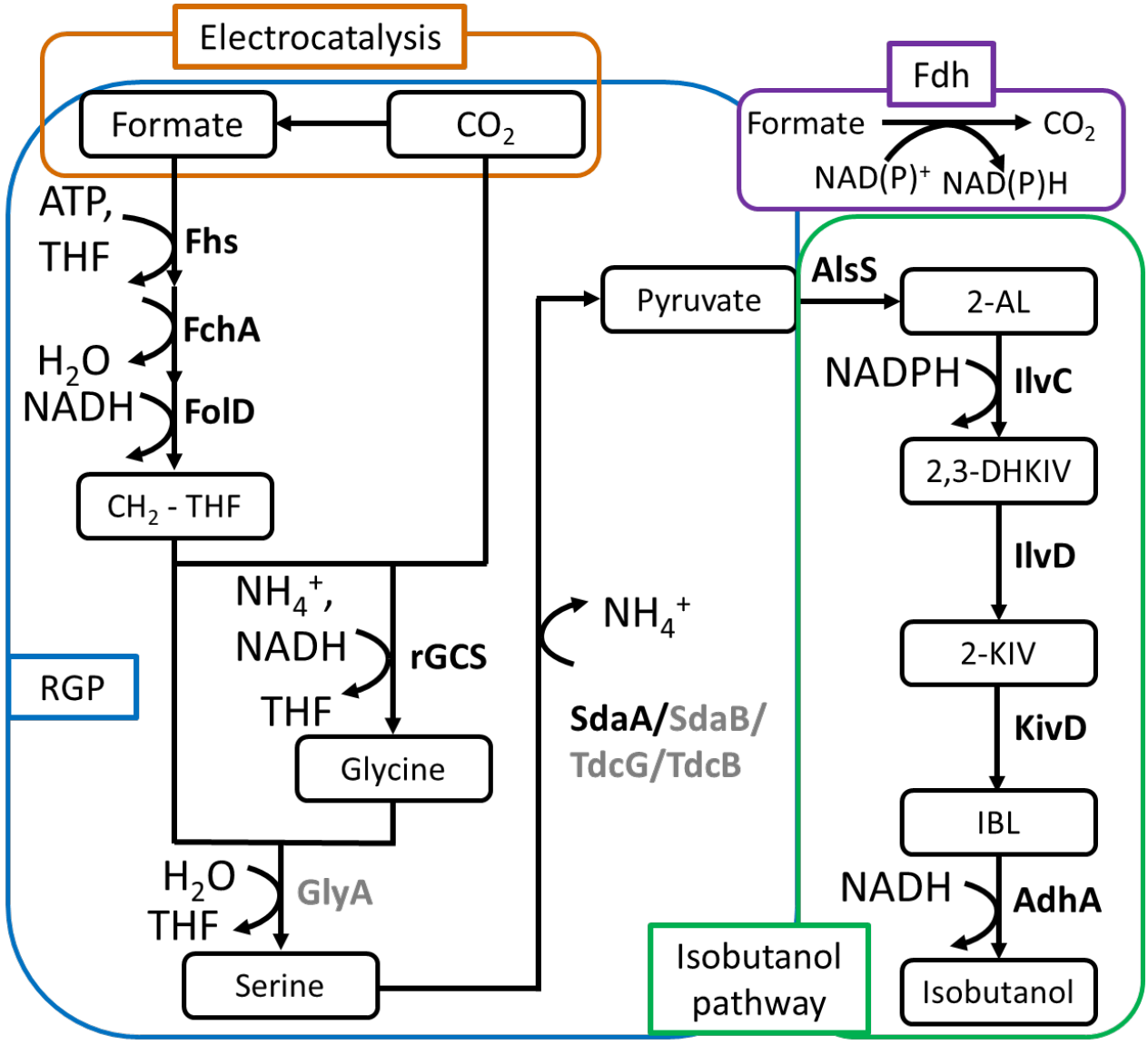


**Figure 1. Isobutanol production pathway in electrical-biological hybrid system.** $CO_2$ is electrocatalytically reduced to formate. Formate is assimilated to methylene-tetrahydrofolate ($CH_2$-THF). The excess $CO_2$ is sequestered by the glycine cleavage system acting in the reverse direction to combine with the $CH_2$-THF to synthesize glycine. Abbreviations: 2-AL (2-acetolactate), 2,3-DHKIV (2,3-dihydroxyketoisovalerate), 2-KIV (2-ketoisovalerate), IBL (Isobutyraldehyde), RGP (Reductive glycine pathway). Enzymes in black are overexpressed in the engineered strain. Enzymes in gray are expressed at native levels.

a)

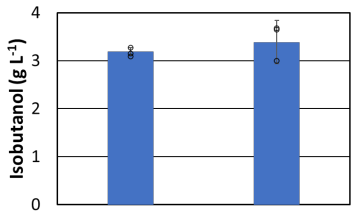


| Strain No. | 3 | 4 |
|---|---|---|
| *serA* | + | - |
| Formate Consumed (g $L^{-1}$) | 0.62 ± 0.03 | 0.51 ± 0.04 |
| Yield (g $g^{-1}$) | 0.34 ± 0.01 | 0.37 ± 0.04 |

b)

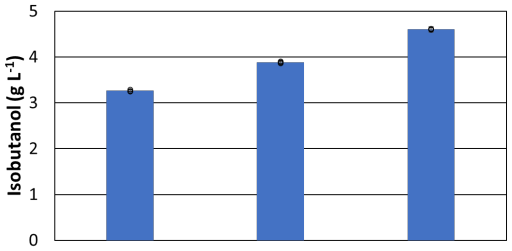


| Strain No. | 5 | 6 | 7 |
|---|---|---|---|
| Fdh | At | Cb | Sc |
| Formate Consumed (g $L^{-1}$) | 1.4 ± 0.06 | 2.5 ± 0.1 | 1.8 ± 0.2 |
| Yield (g $g^{-1}$) | 0.29 ± 0.01 | 0.35 ± 0.03 | 0.22 ± 0.01 |

c)

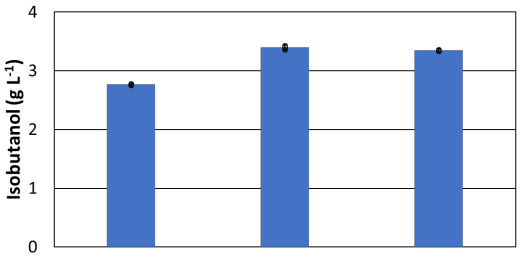


| Strain No. | 4 | 6 | 8 |
|---|---|---|---|
| Formate Consumed (g $L^{-1}$) | 0.05 ± 0.01 | 5.5 ± 0.6 | 5.0 ± 0.9 |
| Yield (g $g^{-1}$) | 0.37 ± 0.06 | 0.39 ± 0.02 | 0.43 ± 0.01 |
| $OD_{600}$ | 33.1 ± 0.5 | 33.3 ± 0.4 | 33.8 ± 0.5 |
| Productivity (g $L^{-1}$ $hr^{-1}$) | 2.8 ± 0.01 | 3.4 ± 0.02 | 3.3 ± 0.01 |

**Figure 2. Isobutanol production in AL17 Strains**

**a)** Isobutanol production in Strains 3 and 4 with the RGP after 2 days. Cultured in M9P with 10 g $L^{-1}$ glucose 3 g $L^{-1}$ formate, 50 mM sodium bicarbonate with 1 mM IPTG and 10 µg $L^{-1}$ aTc. **b)** Isobutanol production after 2 days in Strains 5 through 7 harboring *fdh* variants. Cultured in M9P with 20 g $L^{-1}$ glucose 3 g $L^{-1}$ formate, 50 mM sodium bicarbonate with 1mM IPTG and 10 µg $L^{-1}$ aTc. **c)** High density isobutanol production in Strains 4, 6 and 8. Isobutanol titer reported after 1 h in Strains 4, 6 and 8. Cultured in M9P with 10 g $L^{-1}$ glucose, 10 g $L^{-1}$ formate, 50 mM sodium bicarbonate with 1 mM IPTG and 10 µg $L^{-1}$ aTc. Yield is reported as gram isobutanol produced per gram glucose consumed (g $g^{-1}$). Errors indicate s.d. (n = 3 biological replicates).

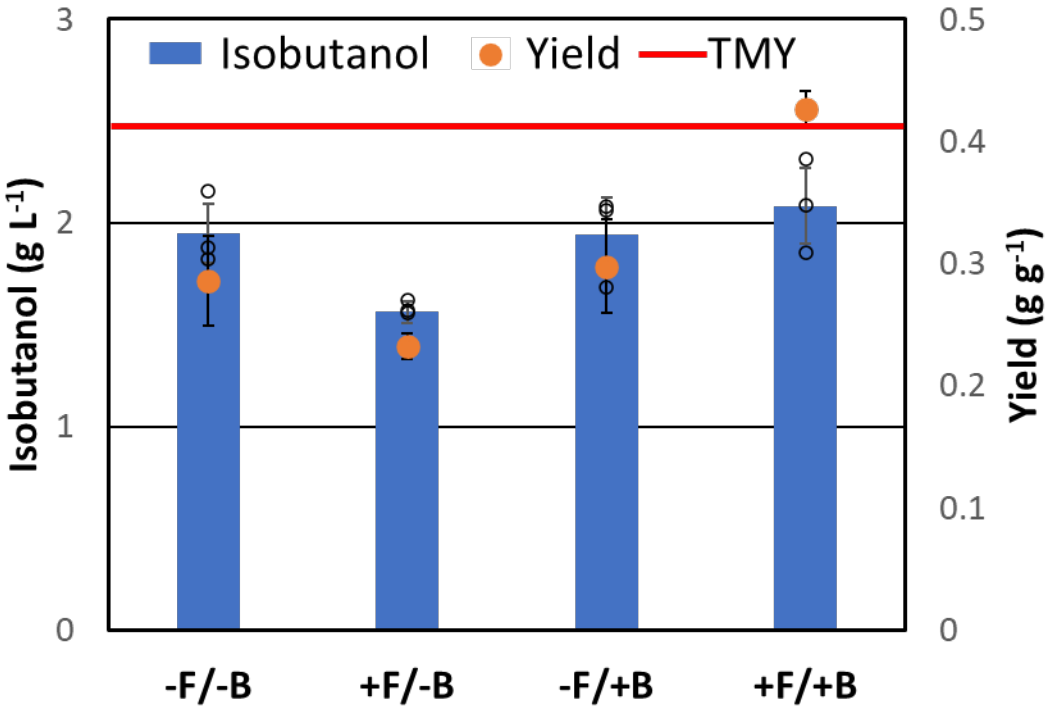


**Figure 3. High density isobutanol titer and yield in Strain 8**

Isobutanol titer after 1 h in Strain 8. Cultured in M9P with 10 g $L^{-1}$ glucose, with or without 3 g $L^{-1}$ formate (+F for with formate, -F for without formate) and 50 mM sodium bicarbonate (+B for with bicarbonate and -B for without bicarbonate). Induced with 1 mM IPTG and 10 µg $L^{-1}$ aTc. Yield is reported as gram isobutanol produced per gram glucose consumed (g $g^{-1}$). The theoretical maximum yield (TMY) is 0.41 g $g^{-1}$. Errors indicate s.d. (n = 3 biological replicates).

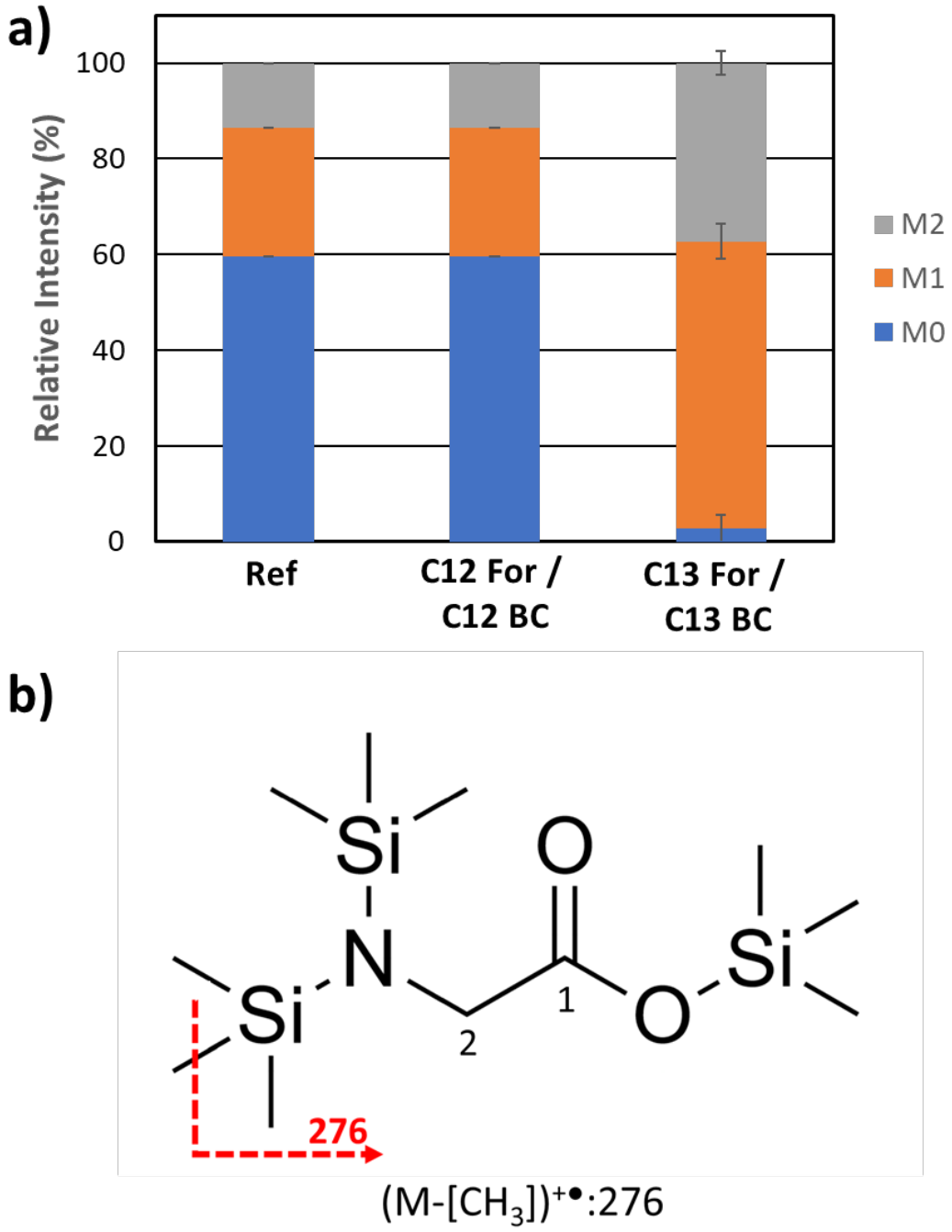


**Figure 4. $^{13}$C-labeling analysis**

**a)** Relative intensity of m/z = 276 (M0), 277 (M1), and 278 (M2) in the glycine produced in Strain 8. Cells were cultured using unlabeled formate and bicarbonate (12For/12BC) or $^{13}$C formate and $^{13}$C bicarbonate (13For/13BC). Ref indicates data from the NIST library of standards. Errors indicate s.d. (n = 3 biological replicates). **b)** Structure of glycine derivatized with MeOX MSTFA. If the pathway is active, position 1 and position 2 would be derived from $CO_2$ and formate, respectively.

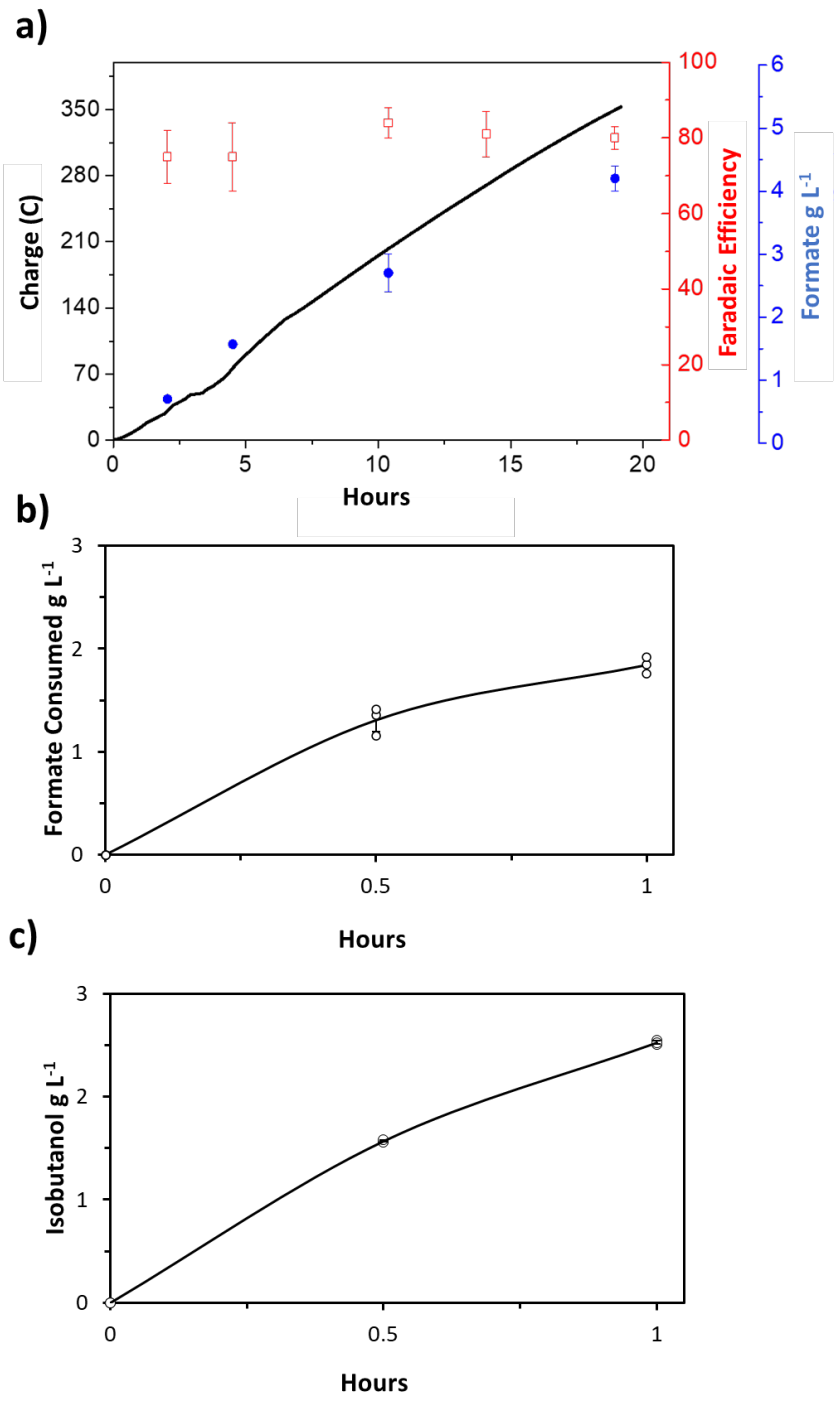


631

632 **Figure 5. Enriched electrochemical broth used for isobutanol synthesis**
633 **a)** Plot of [formate] vs time (blue), Faradic Efficiency vs time (red) and plot of Current density vs
634 time (black) CPE experiment performed with 0.5 mM catalyst in 0.1 M phosphate buffered
635 aqueous solution at pH 7.2. b) *E. coli* formate consumption of electrocatalytically produced
636 formate. c) Isobutanol production in *E. coli* using electrochemical broth. Error bars indicate s.d.
637 (n = 3 technical (a) and biological (b & c) replicates).